Inorg. Chem. **1993,** *32,* 3995–4003

Synthesis and Characterization of Copper(II) Complexes Containing *N*-Glycoside Ligands and Their Use in the Catalytic Epoxidation of Olefins

Tomoaki Tanase,* Keisuke Mano, and Yasuhiro Yamamoto*

Department of Chemistry, Faculty of Science, Toho University, Funabashi-shi, Chiba 274, Japan

Received December 9, 1992[●]

The reaction of copper(II) salts with aldoses and ethylenediamine (en) gave new types of copper(II) complexes containing *N*-glycoside ligands, Cu(*N,N'*-(aldose)$_2$-en)X$_2$ (**3**) (*N,N'*-(aldose)$_2$-en = 1,2-bis(aldosylamino)ethane; aldose = D-glucose, D-mannose, D-xylose, D-lyxose; X = Cl$^-$, Br$^-$). The structure was determined by electronic absorption and circular dichroism spectroscopies, X-ray absorption near edge structure (XANES), and extended X-ray absorption fine structure (EXAFS), in which Cu(hen(OH))X$_2$ (**1**) and Cu(hen(OH)$_2$)X$_2$ (**2**) were used as reference compounds (X = Cl, Br; hen(OH) = 1-amino-2-((2-hydroxyethyl)amino)ethane; hen(OH)$_2$ = 1,2-bis((2-hydroxyethyl)amino)ethane). The complexes **3** have a mononuclear [Cu^{II}N$_2$OX] square planar structure. The *N,N'*-(aldose)$_2$-en moiety acts as a tridentate ligand through the two amino groups and the hydroxy group at the C-2 position of the aldoses. When *N,N'*-dimethylethylenediamine (*N,N'*-Me$_2$en) and *N,N*-dimethylethylenediamine (*N,N*-Me$_2$en) were used, similar copper(II) complexes containing a tridentate *N*-glycoside ligand, Cu(*N*-(aldose)-*N,N'*-Me$_2$en)X$_2$ (**4**) and Cu(*N'*-(aldose)-*N,N*-Me$_2$en)Cl$_2$ (**5**) (aldose = D-glucose, D-mannose; X = Cl$^-$, Br$^-$), were obtained. The sugar complexes **3**–**5** interestingly catalyzed the epoxidation of unfunctionalized olefins ((*E*)-stilbene, (*Z*)-stilbene, (*E*)-β-methylstyrene) with *tert*-butyl hydroperoxide, but the enantioselectivities were low. In contrast, (*E*)-cinnamyl acetate having a polar functional part was converted into its epoxide with an enantiomeric excess of 16%.

Introduction

Carbohydrates have a widespread occurrence in nature and have a number of biological activities in glycoproteins, glycolipids, and antibiotics.[1] The elucidation of interactions between sugars and metals has became an important subject in inorganic chemistry. However, those metal complexes containing carbohydrates that were structurally characterized are very few except for a series of studies by Angyal concerning alkaline earth metal complexes with carbohydrates.[2]

Recently, Yano and Yoshikawa et al. have systematically studied the synthesis and characterization of nickel(II) and cobalt(III) complexes containing *N*-glycosides derived from the reaction of sugars with diamines.[3] As to the nickel(II) complexes using ethylenediamine (en) and trimethylenediamine (tn), it was concluded that an *N*-glycosylamine from an aldose and a diamine coordinates to the nickel atom through the oxygen atom of the hydroxy group at the C-2 position of the sugar moiety and the two nitrogen atoms of the diamine part.[4–7] When *N,N'*-dimethylethylenediamine (*N,N'*-Me$_2$en) was used, the binuclear nickel(II) complex with multidentate *N*-glycosides, 1,2-bis(*N*-methyl-D-mannosylamino)ethane, bridging between the two nickel atoms was obtained and characterized by an X-ray crystallography.[8,9] In the cobalt(III) complexes, *N*-aldosylethylenediamine (aldose = D-mannose, L-rhamnose, D-ribose) attached to the monomeric cobalt center in a tetradentate manner.[10,11] These results suggested that the structure of the sugar complexes can be modified by varying carbohydrates, diamines, and metal ions used. Naturally abundant carbohydrates are easily available as a chiral source in asymmetric reactions; however, reactivities of the sugar complexes were not examined thus far. In particular, the use of these *N*-glycoside complexes in some catalytic reactions remains to be explored.

Here, we prepared and characterized a new series of copper(II) complexes containing *N*-glycoside ligands, in the hope of exploring some catalytic reactions promoted by transition metal–sugar complexes.

Experimental Section

Materials. Dichloromethane and acetonitrile were distilled over calcium hydride. Other reagents were of the best commercial grade and were used without further purification. 1,2-Bis((2-hydroxyethyl)amino)ethane (hen(OH)$_2$), 1-amino-2-((2-hydroxylethyl)amino)ethane (hen(OH)), *tert*-butyl hydroperoxide (3.0 M in 2,2,4-trimethylpentane), and tris[3-((heptafluoropropyl)hydroxymethylene)-(+)-camphorato]europium(III) ([Eu(hfc)$_3$]) were purchased from Aldrich Co., Ltd. [Cu(*N,N,N',N'*-Me$_4$en)$_2$(OH)$_2$]Br$_2$[12] and Cu(hen(OH))X$_2$ (X = Cl$^-$, **1a**, and Br$^-$, **1b**)[13] were prepared by the known methods.

The following abbreviations are used: en, 1,2-diaminoethane; *N,N'*-Me$_2$en, 1,2-bis(methylamino)ethane; *N,N*-Me$_2$en, 1-amino-2-(dimethyl)-ethane; *N,N,N',N'*-Me$_4$en, 1,2-bis(dimethylamino)ethane; D-Glc, D-glucose; D-Man, D-mannose; D-Xyl, D-xylose; D-Lyx, D-lyxose; *N,N'*-(aldose)$_2$-en, 1,2-bis(aldosylamino)ethane; *N*-(aldose)-*N,N'*-Me$_2$en, 1-(methylaldosylamino)-2-(methylamino)ethane; *N'*-(aldose)-*N,N*-Me$_2$en, 1-(dimethylamino)-2-(aldosylamino)ethane.

Measurements. ^{1}H NMR spectra in CDCl$_3$ were obtained at 400 MHz with a JEOL GX-400 superconducting FT spectrometer. Gas

---

[●] Abstract published in *Advance ACS Abstracts,* August 15, 1993.

(1) Kennedy, J. F.; White, C. A. *Bioactive Carbohydrates in Chemistry, Biochemistry and Biology*; John Wiley & Sons: New York, 1983.

(2) Angyal, S. J. *Chem. Soc. Rev.* **1980**, *9*, 415.

(3) Yano, S. *Coord. Chem. Rev.* **1988**, *92*, 113.

(4) Takizawa, S.; Sugita, H.; Yano, S.; Yoshikawa, S. *J. Am. Chem. Soc.* **1980**, *102*, 7969.

(5) Yano, S.; Takizawa, S.; Sugita, H.; Takahashi, K.; Tubomura, T.; Shioi, H.; Yoshikawa, S. *Carbohydr. Res.* **1985**, *142*, 179.

(6) Shioi, H.; Yano, S.; Toriumi, K.; Ito, T.; Yoshikawa, S. *J. Chem. Soc., Chem. Commun.* **1983**, 201.

(7) Yano, S.; Sakai, Y.; Toriumi, K.; Ito, T.; Yoshikawa, S. *Inorg. Chem.* **1985**, *24*, 498.

(8) Tanase, T.; Kurihara, K.; Yano, S.; Kobayashi, K.; Sakurai, T.; Yoshikawa, S. *J. Chem. Soc., Chem. Commun.* **1985**, 1562.

(9) Tanase, T.; Kurihara, K.; Yano, S.; Kobayashi, K.; Sakurai, T.; Hidai, M. *Inorg. Chem.* **1987**, *26*, 3134.

(10) (a) Ishida, K.; Yano, S.; Yoshikawa, S. *Inorg. Chem.* **1986**, *25*, 3552. (b) Ishida, K.; Yashiro, M.; Yano, S.; Hidai, M.; Yoshikawa, S. *J. Am. Chem. Soc.* **1988**, *110*, 2015.

(11) Ishida, K.; Nonoyama, S.; Hirano, T.; Yano, S.; Hidai, M.; Yoshikawa, S. *J. Am. Chem. Soc.* **1989**, *111*, 1599.

(12) Wasson, J. R.; Mitchell, T. P.; Bernard, W. H. *J. Inorg. Nucl. Chem.* **1968**, *30*, 2866.

(13) Ishimura, Y.; Nonaka, Y.; Nishida, Y.; Kida, S. *Bull. Chem. Soc. Jpn.* **1973**, *46*, 3728.

0020-1669/93/1332-3995$04.00/0

Table I. Analytical and Spectral Data for the Copper(II) *N*-Glycosides Complexes **3–5**

complex	formula	anal. data: found (calcd)			yield, %[a]	AB[b]	CD[b]
		C, %	H, %	N, %		λ_{max}, nm (ϵ)[c]	λ_{max}, nm ($\Delta\epsilon$)[c]
$Cu(N,N'\text{-}(\text{D-Glc})_2\text{-en})Cl_2$ (**3a**)	$C_{14}H_{28}N_2O_{10}CuCl_2$	31.87 (32.41)	5.94 (5.44)	5.69 (5.40)	22	726 (82)	750 (0.120) 625 (–0.120) 325 (–0.093)
$Cu(N,N'\text{-}(\text{D-Man})_2\text{-en})Cl_2\cdot 2iPrOH\cdot H_2O$ (**3b**)	$C_{20}H_{46}N_2O_{13}CuCl_2$	36.78 (36.56)	6.73 (7.06)	4.23 (4.26)	23	641 (99)	875 (–0.119) 645 (1.074) 349 (0.313)
$Cu(N,N'\text{-}(\text{D-Xyl})_2\text{-en})Cl_2$ (**3c**)	$C_{12}H_{24}N_2O_8CuCl_2$	31.70 (31.42)	5.63 (5.27)	6.54 (6.11)	35	690 (83)	755 (0.185) 610 (–0.088) 372 (0.070)
$Cu(N,N'\text{-}(\text{D-Lyx})_2\text{-en})Cl_2\cdot H_2O$ (**3d**)	$C_{12}H_{26}O_9N_2CuCl_2$	30.06 (30.23)	5.62 (5.50)	5.34 (5.88)	28	700 (76)	650 (0.476)
$Cu(N,N'\text{-}(\text{D-Glc})_2\text{-en})Br_2\cdot iPrOH\cdot H_2O$ (**3e**)	$C_{17}H_{38}N_2O_{12}CuBr_2$	29.71 (29.77)	5.29 (5.58)	4.78 (4.08)	63	713 (67)	770 (0.196) 595 (–0.261)
$Cu(N,N'\text{-}(\text{D-Man})_2\text{-en})Br_2\cdot iPrOH\cdot EtOH$ (**3f**)[d]	$C_{19}H_{42}N_2O_{12}CuBr_2$	32.07 (31.97)	5.88 (5.93)	4.65 (3.92)	14	632 (94)	850 (–0.056) 620 (0.764)
$Cu(N\text{-}(\text{D-Glc})\text{-}N,N'\text{-}Me_2en)Cl_2\cdot iPrOH\cdot 2H_2O$ (**4a**)	$C_{13}H_{34}N_2O_8CuCl_2$	32.89 (32.47)	6.67 (7.13)	6.19 (5.83)	10	725 (110)	673 (–0.348)
$Cu(N\text{-}(\text{D-Man})\text{-}N,N'\text{-}Me_2en)Cl_2\cdot 2H_2O$ (**4b**)	$C_{10}H_{26}N_2O_7CuCl_2$	29.21 (28.54)	6.06 (6.23)	6.23 (6.66)	12	725 (156)	700 (0.254)
$Cu(N\text{-}(\text{D-Glc})\text{-}N,N'\text{-}Me_2en)Br_2\cdot iPrOH$ (**4c**)	$C_{13}H_{30}N_2O_6CuBr_2$	29.68 (29.25)	5.82 (5.67)	5.40 (5.25)	43	707 (125)	660 (–0.270)
$Cu(N\text{-}(\text{D-Man})\text{-}N,N'\text{-}Me_2en)Br_2\cdot CH_3OH\cdot H_2O$ (**4d**)	$C_{11}H_{28}N_2O_7CuBr_2$	25.48 (25.23)	5.08 (5.39)	5.31 (5.35)	7	707 (178)	725 (0.958)
$Cu(N'\text{-}(\text{D-Glc})\text{-}N,N\text{-}Me_2en)Cl_2\cdot CH_3OH\cdot H_2O$ (**5a**)	$C_{11}H_{28}N_2O_7CuCl_2$	30.79 (30.39)	6.22 (6.49)	6.37 (6.44)	12	724 (130)	760 (0.073) 660 (–0.037) 530 (–0.014)
$Cu(N'\text{-}(\text{D-Man})\text{-}N,N\text{-}Me_2en)Cl_2\cdot CH_3OH$ (**5b**)	$C_{11}H_{26}N_2O_6CuCl_2$	31.17 (31.70)	6.34 (6.29)	6.84 (6.72)	24	704 (107)	640 (0.216)

[a] Based on Cu. [b] In methanol. [c] $mol^{-1}\,dm^3\,cm^{-1}$. [d] Recrystallized from a iPrOH/EtOH/MeOH mixed solvent.

Table II. Crystallographic Data and Experimental Conditions for Complexes **1** and **2**

	complex			
	1a	**1b**	**2a**	**2b**
formula	$C_4H_{12}N_2OCuCl_2$	$C_4H_{12}N_2OCuBr_2$	$C_6H_{16}N_2O_2CuCl_2$	$C_6H_{16}N_2O_2CuBr_2$
mol wt	238.60	327.51	282.66	371.56
cryst size, mm	0.20 × 0.10 × 0.05	0.59 × 0.55 × 0.30	0.30 × 0.25 × 0.25	0.20 × 0.10 × 0.10
cryst system	monoclinic	monoclinic	monoclinic	monoclinic
space group	$P2_1$ (No. 4)	$P2_1$ (No. 4)	$P2_1/c$ (No. 14)	$P2_1/n$ (No. 14)
a, Å	8.272(1)	8.452(9)	8.300(1)	7.413(4)
b, Å	6.110(2)	6.367(7)	10.883(2)	8.307(1)
c, Å	8.7529(6)	8.894(8)	13.232(2)	19.118(4)
β, deg	90.02(2)	90.05(9)	96.75(1)	99.13(3)
V, Å^3	442.4(3)	479(3)	1187.0(3)	1162.4(7)
Z	2	2	4	4
d(calcd), g cm^{-3}	1.791	2.272	1.582	2.123
T, °C	23	23	23	23
μ, mm^{-1}	3.026	10.505	2.274	8.669
2θ range, deg	$6 < 2\theta < 50$	$6 \leq 2\theta < 50$	$6 < 2\theta < 50$	$6 < 2\theta < 50$
no. of data	462 ($I > 3\sigma(I)$)	490 ($I > 3\sigma(I)$)	1156 ($I > 3\sigma(I)$)	1504 ($I > 3\sigma(I)$)
R	0.045	0.054	0.044	0.032
R_w	0.035	0.049	0.042	0.026
GOF	1.92	3.40	1.55	1.74

chromatography was performed on a Shimazu GC-12A using a flame ionization detector. HPLC analysis was performed with a TSK-CCPM system (Toso Co., Ltd.) using a ODS-80TM reversed phase column and a UV-8011 detector. The electronic absorption spectra were measured with a Jasco Ubest-30 spectrophotometer. Circular dichroism spectra were recorded on a Jasco J-500 recording spectropolarimeter, and optical rotations in benzene were measured on a Jasco DIP-360 polarimeter.

Preparation of $Cu(hen(OH)_2)X_2$ ($X = Cl^-, Br^-$) (2). A 2.0-mmol amount of $Hen(OH)_2$ was added to a 40-mL methanolic solution containing 2.0 mmol of $CuX_2\cdot 2H_2O$ (X = Cl, Br). The blue solution was concentrated to ca. 20 mL, and the addition of EtOH gave blue crystals of $Cu(hen(OH)_2)X_2$ (X = Cl (**2a**), Br (**2b**)). Data for **2a** are as follows. Yield: 99%. Anal. Calcd for $C_6H_{16}N_2O_2CuCl_2$: C, 25.50; H, 5.71; N, 9.91. Found: C, 25.21; H, 5.62; N, 9.71. UV–vis (in CH_3OH) [λ_{max} (ϵ)]: 713 nm (107 $mol^{-1}\,dm^3\,cm^{-1}$). Data for **2b** are as follows. Yield: 81%. Anal. Calcd for $C_6H_{16}N_2O_2CuBr_2$: C, 19.40; H, 4.34; N, 7.54. Found: C, 19.47; H, 3.94; N, 7.09. UV–vis (in CH_3OH) [λ_{max} (ϵ)]: 707 nm (138 $mol^{-1}\,dm^3\,cm^{-1}$).

Preparation of $Cu(N,N'\text{-}(aldose)_2\text{-}en)X_2\cdot Solv$ (3). A representative procedure is described as follows: A 2.5-mmol amount of ethylenediamine dissolved in 10 mL of methanol was added to a solution of D-Glc (5.0 mmol) in 30 mL of methanol in the presence of a small amount of NH_4Cl (0.6 mmol). The solution was incubated at 60 °C for 1 h until the color of the solution turned pale yellow. Then, 2.5 mmol of $CuX_2\cdot 2H_2O$ ($X = Cl^-$) was added to the solution, which was allowed to stand at room temperature for 30 min; the color of the solution changed from blue to bluish green. The solution was concentrated to about 20 mL by a rotary evaporator, loaded onto a Sephadex LH-20 gel permeation column, and eluted with methanol. The bluish green eluate was concentrated to about 10 mL, and an addition of iPrOH gave a bluish green precipitate of $Cu(N,N'\text{-}(\text{D-Glc})_2\text{-en})Cl_2$ (**3a**), which was recrystallized from a mixed solvent of MeOH and iPrOH (yield 22%). The analytical and spectral data are listed in Table I. $Cu(N,N'\text{-}(\text{D-Man})_2\text{-en})Cl_2\cdot 2iPrOH\cdot H_2O$ (**3b**), $Cu(N,N'\text{-}(\text{D-Xyl})_2\text{-en})Cl_2$ (**3c**), $Cu(N,N'\text{-}(\text{D-Lyx})_2\text{-en})Cl_2\cdot H_2O$ (**3d**), $Cu(N,N'\text{-}(\text{D-Glc})_2\text{-en})Br_2\cdot iPrOH\cdot H_2O$ (**3e**), and $Cu(N,N'\text{-}(\text{D-Man})_2\text{-en})Br_2\cdot iPrOH\cdot EtOH$ (**3f**) were obtained by the similar procedure (Table I). The presence of solvated molecules were also checked by GC.

Preparation of $Cu(N\text{-}(aldose)\text{-}N,N'\text{-}Me_2en)X_2\cdot Solv$ (4) and $Cu(N'\text{-}(aldose)\text{-}N,N\text{-}Me_2en)Cl_2\cdot Solv$ (5). A 2.5-mmol amount of $N,N'\text{-}Me_2en$ was added to a solution of aldose (2.5 mmol) in 30 mL of MeOH in the presence of a small amount of NH_4Cl (0.6 mmol), and the solution was incubated at 60 °C for 1 h. Then, 2.5 mmol of $CuCl_2\cdot 2H_2O$ was added to the solution, which was allowed to stand at room temperature for 30 min. The resultant solution was chromatographed on Sephadex LH-20 gel to give a bluish green precipitate of $Cu(N\text{-}(\text{D-Glc})\text{-}N,N'\text{-}Me_2en)Cl_2\cdot iPrOH\cdot 2H_2O$ (**4a**), which was recrystallized from a mixture of MeOH and iPrOH (yield 10%). The analytical and spectral data are given in Table I. $Cu(N\text{-}(\text{D-Man})\text{-}N,N'\text{-}Me_2en)Cl_2\cdot 2H_2O$ (**4b**), $Cu(N\text{-}(\text{D-Glc})\text{-}N,N'\text{-}Me_2en)Br_2\cdot iPrOH$ (**4c**), $Cu(N\text{-}(\text{D-Man})\text{-}N,N'\text{-}Me_2en)Br_2\cdot CH_3OH\cdot H_2O$ (**4d**), $Cu(N'\text{-}(\text{D-Glc})\text{-}N,N\text{-}Me_2en)Cl_2\cdot CH_3OH\cdot H_2O$ (**5a**), and

Scheme I

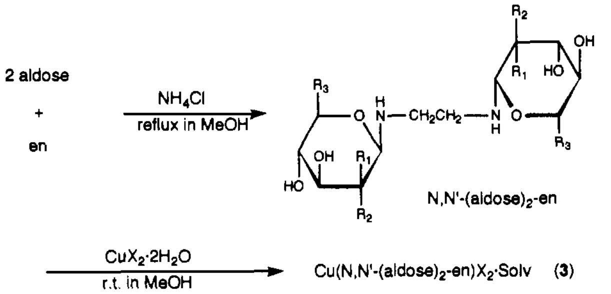

3a; $R_1 = H$, $R_2 = OH$, $R_3 = CH_2OH$, $X = Cl$
3b; $R_1 = OH$, $R_2 = H$, $R_3 = CH_2OH$, $X = Cl$
3c; $R_1 = H$, $R_2 = OH$, $R_3 = H$, $X = Cl$
3d; $R_1 = OH$, $R_2 = H$, $R_3 = H$, $X = Cl$
3e; $R_1 = H$, $R_2 = OH$, $R_3 = CH_2OH$, $X = Br$
3f; $R_1 = OH$, $R_2 = H$, $R_3 = CH_2OH$, $X = Br$

Cu(*N*′-(D-Man)-*N*,*N*-Me$_2$en)Cl$_2$·CH$_3$OH (**5b**) were prepared by the similar method (Table I). The complexes **4** and **5** could be also prepared by the reaction of Cu(*N*,*N*′-Me$_2$en)Cl$_2$ or Cu(*N*,*N*-Me$_2$en)Cl$_2$[14] with an excess amount of aldoses in refluxing methanol.

X-ray Crystallographic Analyses of 1a,b and 2a,b. Crystal Data. Crystal data and experimental conditions for **1a,b** and **2a,b** are listed in Table II. The intensity data were collected on a Rigakudenki AFC5S four-circle automated diffractometer. The three standard reflections were monitored every 150 reflections for each compound, showing no systematic decrease in intensity. The standard Lorentz, polarization, and absorption corrections were applied. The crystal **1b** was cut to an appropriate size.

Structure Solution and Refinement. Compounds 1a,b. The structures were solved by direct methods (MITHRIL),[15] and the positions of the Cu and Cl (or Br) atoms were determined from the initial *E* map. The coordinates of the remaining non-hydrogen atoms were deduced by means of alternate cycles of difference Fourier syntheses and full-matrix least-squares refinements. Atomic scattering factors were taken from ref 16. The positions of hydrogen atoms except for N–H were calculated by assuming a tetrahedral coordination about the carbon atoms with a C–H bond distance of 0.95 Å. Finally, all non-hydrogen atoms were refined with anisotropic temperature factors (hydrogen atoms were not refined) to $R = \Sigma||F_o| - |F_c||/\Sigma|F_o| = 0.045$ and $R_w = (\Sigma_w(|F_o| - |F_c|)^2/\Sigma w|F_o|^2)^{1/2} = 0.035$ ($w = 1/\sigma^2(F_o)$) for **1a** and $R = 0.054$ and $R_w = 0.049$ for **1b**. The absolute configurations of the complex cations were not determined.

Compounds 2a,b. The coordinates of Cu and Cl (or Br) were determined from the initial *E* map, and the subsequent Fourier syntheses and full-matrix least-squares techniques gave the positions of the remaining non-hydrogen atoms. The coordinates of hydrogen atoms were determined by difference Fourier syntheses. Final refinement with anisotropic thermal parameters for non-hydrogen atoms and isotropic temperature factors for hydrogen atoms converged to $R = 0.044$ and $R_w = 0.042$ ($w = 1/\sigma^2(F_o)$) for **2a** and $R = 0.032$ and $R_w = 0.026$ for **2b**.

All calculations were performed on a Digital Vax station 3100 M38 computer with TEXSAN-TEXRAY Structure Analysis Package (Molecular Structure Corp.). The perspective views were drawn by using the programs PLUTO[17a] and ORTEP.[17b]

Measurement of X-ray Absorption Spectra. Beam line 10B at the Photon Factory of the National Laboratory for High Energy Physics[18] (2.5 GeV, 340–300 mA) was used with a Si(311) channel-cut monochromator. The experiments were done in the transition mode on boron nitride pellets. In order to avoid higher harmonics contamination, the maximum absorbance measured by this system was kept less than 4. Under such conditions, the amount of higher harmonics X-rays detected by a solid-state detector is less than 0.2% of the fundamental X-rays.[19] The absorption spectra, $\mu x = \ln(I_0/I)$, where μx is the total absorption, were recorded as a function of the X-ray photon energy *E*, with an integration time of 1–2 s/point at room temperature, 800 steps covering the K edge for Cu (8280–10470 eV); the XANES region (8920–9080 eV) was covered with 440 steps, and EXAFS range (9080–9780 eV) was covered with 270 steps. Samples measured were **1a,b**, **2a,b**, and [Cu(*N*,*N*,*N*′,*N*′-Me$_2$en))$_2$(OH)$_2$]Br$_2$ (**6**) as reference compounds together with sugar complexes **3**–**5**. The absorption spectra of methanolic solution samples (0.1 M) for **1**, **2**, **3a,e**, and **4a,c** were measured with a polystyrene cell (l = 1 cm) at room temperature.

Extended X-ray Absorption Fine Structure (EXAFS) Analysis. The extended X-ray absorption spectrum is derived from the absorption spectrum above the Cu K edge, E_0 = 8984 eV. $\mu(\mathbf{k})$ is the absorption coefficient as a function of **k**, the photoelectron wave vector defined as $\mathbf{k} = [(2m/\hbar^2)(E - E_0)]^{1/2}$. After conversion of *E* into photoelectron wave vector **k**, the data were multiplied by $\mathbf{k}^3$ and the modulation of the absorption coefficient, $\chi(\mathbf{k}) = (\mu - \mu_0)/\mu_0$, was obtained by removing a cubic spline background fit to the data with four sections each of $\Delta\mathbf{k}$ = 4.0 A^{-1}, normalized with the edge jump and corrected for the μ_0 dropoff via Victoreen's true absorption. The theoretical expression of the obtained $\mathbf{k}^3\chi(\mathbf{k})$ for the case of single scattering is[20]

$$\mathbf{k}^3\chi(\mathbf{k}) = \sum_i (\mathbf{k}^2 N_i/r_i^2) S_i F_i(\mathbf{k}) \exp(-2\sigma_i^2\mathbf{k}^2) \sin(2\mathbf{k}r_i + \Phi_i(\mathbf{k}))$$

where r_i, N_i, S_i, $F_i(\mathbf{k})$, $\Phi_i(\mathbf{k})$, and σ_i represent the interatomic distance, the coordination number, the reducing factor, the backscattering amplitude, the phase shift, and the Debye–Waller factor, respectively. The backscattering amplitude $F_i(\mathbf{k})$ and the phase shift $\Phi_i(\mathbf{k})$ functions employed were the theoretical curves tabulated by Teo and Lee.[21,22] Four parameters, N_i, r_i, $E_{0i}{}^{\mathrm{p}}$ (=8984 eV − ΔE_i), and σ_i, were varied in the nonlinear least-squares refined curve fitting, and the fixed reducing factors S_i obtained from the analysis of model compounds were used. All calculation were performed on a HITAC S-800 computer at the Computer Center of the University of Tokyo with the systematic programs EXAFS1.[23]

Catalytic Epoxidation of Olefins. A typical procedure for the catalytic epoxidation of olefin is as follows. To an acetonitrile solution (30 mL) containing 1.0 mmol of olefin ((*E*)-stilbene, (*Z*)-stilbene, (*E*)-β-methylstyrene, (*E*)-cinnamyl acetate), 0.02 mmol of copper(II) complex of *N*-glycoside, and bromobenzene as an internal standard was added 2.0 mmol of *tert*-butyl hydroperoxide (2,2,4-trimethylpentane solution). The solution was stirred at room temperature under a nitrogen atmosphere and was monitored with HPLC ((*E*)/(*Z*)-stilbene) and GC (other olefins) by periodically sampling the reaction mixture. After the reaction was over, saturated aqueous Na$_2$SO$_3$ and diethyl ether were added to the solution. The epoxide was isolated by chromatography of the organic layer on silica gel. The absolute configuration and enantiomeric excess (ee) of the epoxide were determined by polarimetric measurement and ^{1}H NMR measurement using chiral shift reagent tris[3-((heptafluoropropyl)hydroxymethylene)-(+)-camphorato]europium(III), [Eu(Hfc)$_3$],[24] respectively.

Results and Discussion

Preparations of Copper(II) Complexes Containing *N*-Glycoside Ligands. D-Glucose (2 equiv) was treated with ethylenediamine (1 equiv) in the presence of a small amount of NH$_4$Cl (0.24 equiv) in refluxing methanol for 1 h, and then CuCl$_2$·2H$_2$O (1 equiv) was added to the solution and allowed to stand at room temperature for 30 min. The solution was chromatographed on a Sephadex LH-20 gel permeation column to give bluish green microcrystals of copper(II) complex (**3a**) in a yield of 22%. The reaction conditions dramatically influenced the yield of **3a**; without refluxing, **3a** was not obtained, whereas, with an extended refluxing time over 1 h, the yield of **3a** decreased owing to Browning reactions

---

(14) Nasanen, R.; Luuklonen, E.; Palonen, H.; Sivonen, M. *Suom. Kemistil. B* **1971**, *44*, 93.
(15) Gilmore, C. J. MITHRIL: an integrated direct methods computer program. University of Glasgow, Scotland. *J. Appl. Crystallogr.* **1984**, *17*, 42.
(16) Cromer, D. T.; Eaber, J. T. *International Tables for X-ray Crystallography*; The Kynoch Press: Birmingham, England, 1974; Vol. IV.
(17) (a) Motherwell, S.; Clegg, W. PLUTO: Program for Plotting Molecular and Crystal Structures. University of Cambridge, England, 1978. (b) Johnson, C. K. ORTEP II, Oak Ridge National Laboratory, Oak Ridge, TN, 1976.
(18) *Photon Factory Activity Report*; National Laboratory for High Energy Physics: Ibaraki, Japan, 1986; No. 3.
(19) Nomura, M. *KEK Reports*; National Laboratory for High Energy Physics: Ibaraki, Japan, 1985; No. 85-7.
(20) Sayers, D. E.; Stern, E. A.; Lytle, F. W. *Phys. Rev. Lett.* **1971**, *27*, 1204.
(21) Teo, B. K.; Lee, P. A.; Simons, A. L.; Eisenberger, P.; Kincaid, B. M. *J. Am. Chem. Soc.* **1977**, *99*, 3854.
(22) Teo, B. K.; Lee, P. A. *J. Am. Chem. Soc.* **1979**, *101*, 2815.
(23) Kosugi, N.; Kuroda, H. *Program EXAFS1*; Research Center for Spectrochemistry, University of Tokyo: Tokyo, Japan, 1985.
(24) Groves, J. T.; Myers, R. S. *J. Am. Chem. Soc.* **1983**, *105*, 5971.

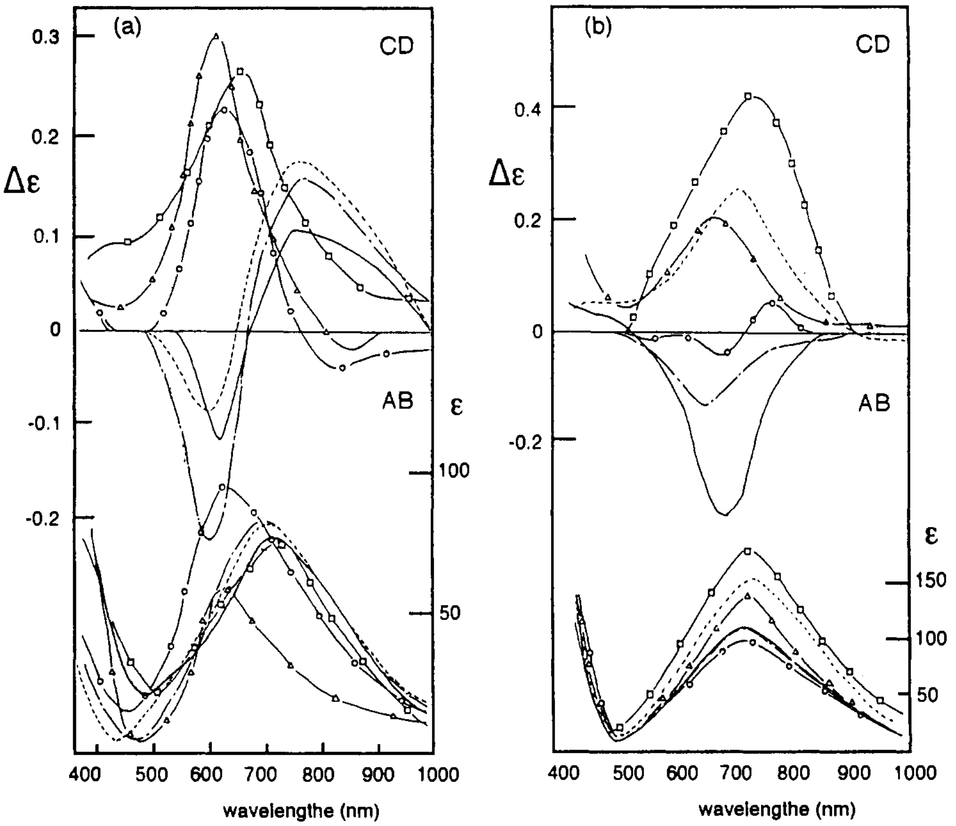

Figure 1. AB and CD spectra: (a) Copper(II) complexes of *N*-glycosides (**3**) (— (**3a**), – O – (**3b**), - - - (**3c**), – ■ – (**3d**), – – – (**3e**), – tuo – (**3f**)); (b) copper(II) complexes **4** and **5** (— (**4a**), - - - (**4b**), – – – (**4c**), – □ – (**4d**), – O – (**5a**), – △ – (**5b**)).

or degradations of D-glucose.[25,26] Analytical data for **3a** showed the complex consisted of one ethylenediamine and two carbohydrate moieties for every one copper atom (Table I). In the IR spectrum, besides a broad band for the hydroxyl groups, a moderate peak corresponding to δ_{N-H} was observed at 1610 cm^{-1}, which was shifted to the high-energy side compared with those of free ethylenediamine and Cu(II)–ethylenediamine complexes, suggesting that an *N*-glycosidic bond formation took place. Generally, *N*-aldosylamines are easily prepared by direct interaction of aldoses with primary and secondary aliphatic amines, and *N*-aldosylamines are known to adopt the β-anomeric form.[26] Furthermore, it has been revealed that *N*-(D-glucosyl)ethylenediamine or -trimethylenediamine was smoothly derived from the reaction of Ni(II) complexes of corresponding diamines with aldoses and attached to the metal center with the β-anomeric form.[3–9] From these, complex **3a** was expected to contain a 1,2-bis(β-D-glucosylamino)ethane ligand, *N,N'*-(D-Glc)$_2$-en, which was formed from the reaction of D-glucose with en as shown in Scheme I. The intermediate *N,N'*-(D-Glc)$_2$-en was too hygroscopic to be isolated.

When D-mannose, D-xylose, and D-lyxose were used as a sugar part, similar copper(II) complexes formulated as Cu(*N,N'*-(aldose)$_2$-en)Cl$_2$·Solv (**3b–d**) (Solv = solvents of crystallization) were obtained (Table I). Cu(*N,N'*-(aldose)$_2$-en)Br$_2$·Solv (aldose = D-Glc (**3e**), D-Man (**3f**)) were also prepared by the reaction of CuBr$_2$·2H$_2$O with the corresponding *N,N'*-(aldose)$_2$-en generated from aldose and en in *situ*.

Electronic absorption (AB) and circular dichroism (CD) spectra of the complexes **3** in methanol are presented in Figure 1a, and the spectral data are summarized in Table I. The spectra of these complexes exhibited one pseudosymmetrical broad band centered in the 600–750-nm region, which is characteristic of square planar copper(II) complexes.[27] The CD spectra showed conspicuous Cotton effects in the d–d transition region (500–900 nm) and strongly indicated the coordination of sugar moieties to the metal center. Further, the CD spectral patterns were divided into two groups; the spectra of the glucose-type aldoses (D-Glc, D-Xyl) having an *R* configuration about the C-2 carbon showed (–) peaks around 600 nm, and those of the mannose-type aldoses (D-Man, D-Lyx) having an S configuration about the C-2 carbon indicated intense (+) peaks, probably suggesting the presence of the coordination of the hydroxy group on the C-2 carbon of carbohydrate. Further, the bimodal shape of peaks in **3a,c,e** may indicate an "exiton coupling"[28] probably arising from a rapid equilibrium in which both sugar moieties interact with the metal center alternatively.

When *N,N'*-Me$_2$en and *N,N*-Me$_2$en were used instead of en, bluish green complexes containing sugar moieties, Cu(*N*-(aldose)-*N,N'*-Me$_2$en)X$_2$·Solv (**4**) and Cu(*N'*-(aldose)-*N,N*-Me$_2$en)-Cl$_2$·Solv (**5**) were obtained as microcrystals (Table I). Analytical and IR spectral data (ν_{OH} 3700–3050, δ_{NH} 1650–1600 cm^{-1}) indicated that the complexes **4** and **5** contained a *N*-glycoside ligand derived from one diamine molecule and one aldose unit (Scheme II). Similar types of 1:1 *N*-glycoside ligands have been already observed in the nickel(II) complexes.[3] Formally, the reaction of *N,N'*-Me$_2$en with 2 equiv of aldose can give *N,N'*-bis(D-glycosyl)diamine (*N,N'*-(aldose)$_2$-*N,N'*-Me$_2$en), but such complexes Cu(*N,N'*-(aldose)$_2$-*N,N'*-Me$_2$en)X$_2$ were not obtained even by using an excess amount of aldoses, probably due to the lability of C–N glycosidic linkage owing to the effect of *N*-methyl groups. Since the AB and CD spectral patterns of **4** and **5** were similar to those of complexes **3** (Figure 1b and Table I), coordination of the hydroxy group on the C-2 carbon of the sugar moiety could be also expected.

---

(25) Maillard, L. C. C. R. *Hebd. Seances Acad. Sci.* **1912**, *154*, 66.
(26) Paulsen, H.; Pflughaupt, K. W. *Carbohydrates, Chemistry and Biochemistry*; Academic: New York, 1980; Vol. 1B.
(27) Zimmerman, D. N.; Hall, J. L. *Inorg. Chem.* **1973**, *12*, 2616.
(28) Harada, N.; Nakanishi, K. *Circular Dichroic Spectroscopy: Exiton Coupling in Organic Stereochemistry*; University Science Books: Mill Valley, CA, 1983.

Scheme II

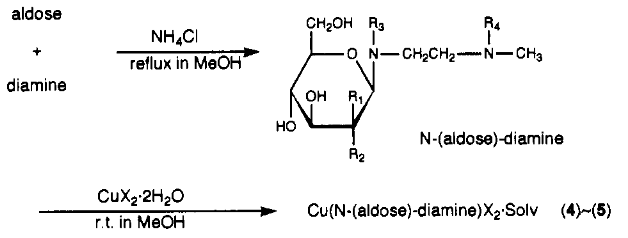

4a; $R_1 = H$, $R_2 = OH$, $R_3 = CH_3$, $R_4 = H$, $X = Cl$
4b; $R_1 = OH$, $R_2 = H$, $R_3 = CH_3$, $R_4 = H$, $X = Cl$
4c; $R_1 = H$, $R_2 = OH$, $R_3 = CH_3$, $R_4 = H$, $X = Br$
4d; $R_1 = OH$, $R_2 = H$, $R_3 = CH_3$, $R_4 = H$, $X = Br$
5a; $R_1 = H$, $R_2 = OH$, $R_3 = H$, $R_4 = CH_3$, $X = Cl$
5b; $R_1 = OH$, $R_2 = H$, $R_3 = H$, $R_4 = CH_3$, $X = Br$

The copper(II) sugar complexes (**3–5**) were highly hygroscopic, and no single crystal suitable for an X-ray crystallography was obtained. It is difficult to assign further detailed structures from only AB, CD, and IR spectral data. So, in order to obtain direct structural information around the metal center, we have undertaken an XAFS (X-ray absorption fine structure) analysis of the copper(II) complexes of *N*-glycosides in both the solid and solution states (*vide infra*).

X-ray Analyses of Cu(hen(OH))X$_2$ (1) and Cu(hen(OH)$_2$)X$_2$ (2). In the attempt to undertake the XAFS analysis of the sugar complexes (**3–5**), we investigated the X-ray crystallographic and XAFS analyses of Cu(hen(OH))X$_2$ (X = Cl (**1a**), Br (**1b**)) and Cu(hen(OH)$_2$X$_2$ (X = Cl (**2a**), Br (**2b**)) as their model compounds. It has been reported that hen(OH) and hen(OH)$_2$ form various 1:1 and 2:1 complexes with Cu^{2+} ion in solution, the structures of which varied depending on their counteranions and pH conditions.[13,29,30] However, only a few studies have been reported on structures of crystalline copper(II) complexes of these ligands.[13,31]

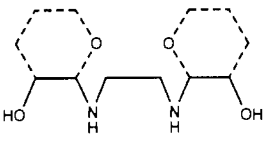

hen(OH)$_2$

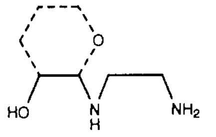

hen(OH)

*The dashed-line parts represent the sugar moieties of analogous N-glycoside ligands.

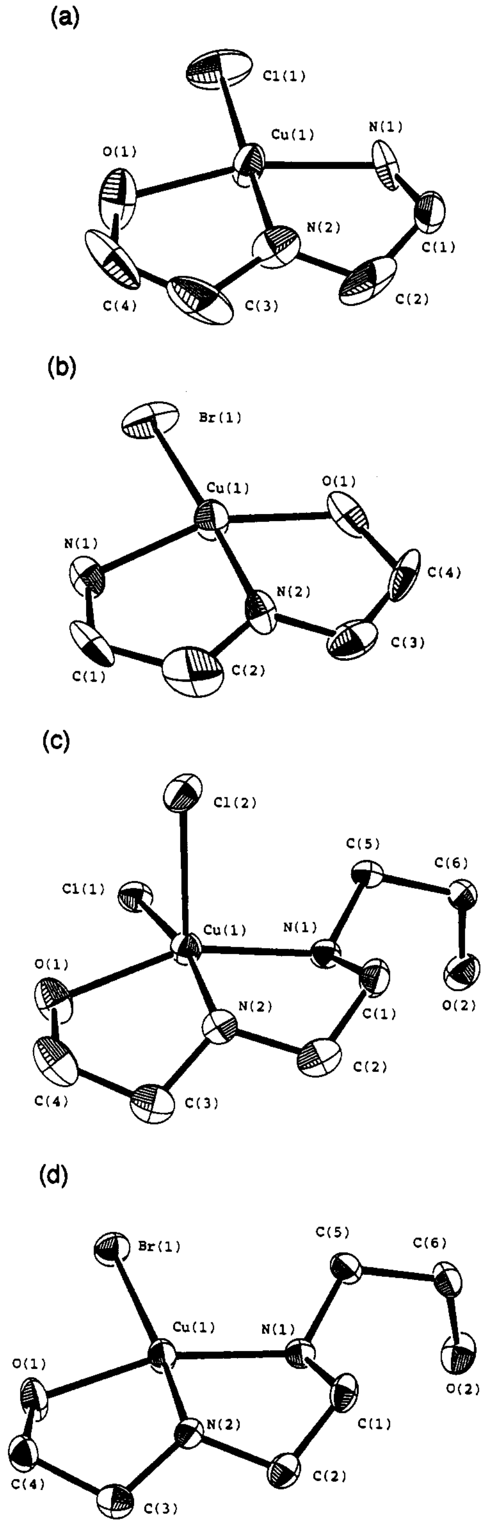

Figure 2. Perspective drawings with the atomic numbering scheme for (a) Cu(hen(OH))Cl$_2$ (**1a**), (b) Cu(hen(OH))Br$_2$ (**1b**), (c) Cu(hen(OH)$_2$)-Cl$_2$ (**2a**), and (d) Cu(hen(OH)$_2$)Br$_2$ (**2b**).

Perspective drawings of the complexes, **1a,b** and **2a,b**, with the atomic numbering schemes are given in Figure 2, and some selected interatomic distances and angles are listed in Table III. The coordination geometry around the Cu atom of **1a** is essentially square planar, and the Cu atom is occupied by two N and one O atoms of the hen(OH) ligand and a Cl atom (Cu–Cl(1) = 2.206(3) Å) (Figure 2a). The bite angles of N(1)–Cu–N(2) and N(2)–Cu–O(1) are 83.5(4) and 84.0(4)°, and the *trans* angle of N(1)–Cu–O(1) is 164.7(7)°, which is smaller than the ideal value of 180°, suggesting the presence of strains in this tridentate chelation system. Complex **1b** has a structure isomorphous to that of complex **1a** (Figure 2b). The bond length of Cu–Br(1) is 2.358(5) Å, and the *trans* angle of N(1)–Cu–O(1) is 158(1)°. In the crystal packing of **1a** and **1b**, two counteranions weakly occupy the axial positions (Cu···Cl = 3.08(1), 3.11(1) Å for **1a** and Cu···Br = 3.12(1), 3.31(1) Å for **1b**), resulting in a chain structure along the *b* axis as depicted in Figure 3a,b.[32] The complex cation of **2b** has a square planar structure similar to that of **1b**. The central copper is coordinated by a bromide ion (Cu–

---

(29) Courtney, R. C.; Gustafson, R. L.; Chaberek, S., Jr.; Martell, A. E. *J. Am. Chem. Soc.* **1959**, *81*, 519.

(30) Hughes, M. N.; Underhill, M.; Rutt, K. J. *J. Chem. Soc., Dalton Trans.* **1972**, 1219.

(31) Cu(hen(OH))$_2$Cl$_2$ and Cu(hen(OH))$_2$(ClO$_4$)$_2$ were revealed to have a distorted octahedral structure; the former contained the apical coordination of two chloride ions (Pajunen, A.; Nasakkala, M. *Suom. Kemistil. B* **1972**, *45*, 47), and the latter contained that of two alcoholic oxygen atoms (Chastain, R. V., Jr.; Dominick, T. L.; *Inorg. Chem.* **1973**, *12*, 2621). In contrast, the 1:1 complexes Cu(hen(OH))X$_2$ and Cu(hen(OH)$_2$)X$_2$ have not been structurally characterized yet, although Nasanen et al. tried an X-ray crystallographic study (Nasanen, R.; Lemmetti, L.; Anttila, K.; Lehtinen, K.; Mannula, M. *Suom. Kemistil. B* **1969**, *42*, 357). After that, Kida et al. proposed that Cu(hen(OH))-Cl$_2$ had a square planar structure with two chloride ions and two amino nitrogen atoms, the alcoholic hydroxy group being not likely to form a distinct bond with the metal ion, by UV, IR, and ESR spectroscopies.[13]

(32) Supplementary material.

Table III. Selected Bond Lengths and Angles of **1** and **2**[a]

1a		**1b**		**2a**		**2b**	
			Bond Lengths (Å)				
Cu–Cl(1)	2.206(3)	Cu–Br(1)	2.358(5)	Cu–Cl(1)	2.272(2)	Cu–Br(1)	2.372(1)
Cu–N(1)	2.005(8)	Cu–N(1)	1.98(2)	Cu–N(1)	2.023(5)	Cu–N(2)	1.994(4)
Cu–N(2)	1.952(7)	Cu–N(2)	1.96(1)	Cu–N(2)	2.012(6)	Cu–N(1)	2.010(4)
Cu–O(1)	1.992(8)	Cu–O(1)	2.03(1)	Cu–O(1)	2.056(5)	Cu–O(1)	1.985(4)
				Cu–Cl(2)	2.513(2)		
			Bond Angles (deg)				
Cl(1)–Cu–N(2)	179.1(7)	Br(1)–Cu–N(2)	175(2)	Cl(1)–Cu–N(2)	165.0(2)	Br(1)–Cu–N(2)	169.7(1)
Cl(1)–Cu–N(1)	95.8(3)	Br(1)–Cu–N(1)	94.7(5)	Cl(1)–Cu–N(1)	97.7(2)	Br(1)–Cu–N(1)	101.5(1)
Cl(1)–Cu–O(1)	96.7(3)	Br(1)–Cu–O(1)	95.3(4)	Cl(1)–Cu–O(1)	90.4(1)	Br(1)–Cu–O(1)	93.2(1)
N(1)–Cu–N(2)	83.5(4)	N(1)–Cu–N(2)	83.9(7)	N(1)–Cu–N(2)	85.2(2)	N(1)–Cu–N(2)	85.4(2)
N(2)–Cu–O(1)	84.0(4)	N(2)–Cu–O(1)	84.5(6)	N(2)–Cu–O(1)	81.7(2)	N(2)–Cu–O(1)	81.5(2)
N(1)–Cu–O(1)	164.7(7)	N(1)–Cu–O(1)	158(1)	N(1)–Cu–O(1)	156.6(2)	N(1)–Cu–O(1)	162.2(2)
				Cl(1)–Cu–Cl(2)	98.32(7)		
				Cl(2)–Cu–N(2)	95.7(2)		
				Cl(2)–Cu–N(1)	98.6(2)		
				Cl(2)–Cu–O(1)	101.9(2)		

[a] Estimated standard deviations in parentheses.

Br(1) = 2.372(1) Å) and a tridentate hen(OH)$_2$ ligand via the two nitrogen atoms of the amino groups and the one oxygen atom of the hydroxy group (N(1)–Cu–O(1) = 162.2(2)°), the other hydroxy group not participating in the coordination system (Figure 2d). The two axial sites are semicoordinated by a outer bromide anion (3.244(1) Å) and the bromine atom of another molecule (3.320(1) Å) as shown in Figure 3d, apparently forming a dimeric structure. Complex **2a** has a square pyramidal structure; a chloride ion (Cu–Cl(1) = 2.272(2) Å) and a tridentate hen(OH)$_2$ ligand are included in the equatorial plane, and the axial site is occupied by another chloride ion (Cu–Cl(2) = 2.513(2) Å) (Figure 2c). The coordination pattern of hen(OH)$_2$ is very similar to that found in **2b**. The vacant axial site is semicoordinated by the equatorial chlorine atom of another molecule (Cu···Cl = 3.544(2) Å) (Figure 3c).[32] The square pyramidal structure of **2a** can be viewed as one of the most distorted forms from the square planar geometry as observed in **2b**.

X-ray absorption spectra around the Cu K edge of **1** and **2** in both the solid and solution states were measured as reference compounds to examine the reliability of our EXAFS analyses for copper(II) complexes containing *N*-glycosides. The Fourier transforms of raw data (solid state) are presented in Figure 4, and the structural parameters derived from the curve-fitting analyses are listed in Table IV.[32] The Fourier transform of **1b** showed three peaks at about 1.6, 1.9–2.2, and 2.5–2.7 Å (before phase-shift correction), which were attributable to the nitrogen and oxygen atoms in the first shell, the coordinated bromine atom, and the carbon atoms in the chelation rings, respectively (Figure 4a). These peaks were back-Fourier transformed by the use of a proper window (ca. 1–3 Å) to produce an abstracted EXAFS oscillation subjected to the curve-fitting analysis by using a three-term equation of $k^3\chi_{calcd}(k) = k^3[\chi_{N/O}(k) + \chi_{Br}(k) + \chi_C(K)]$ (Figure 5).[32] For the Fourier transforms of **1a** and **2b**, similar curve-fitting techniques were applied. The structural parameters of **1a,b** and **2b** derived from EXAFS analyses in the solid state are in good agreement with those from their X-ray crystallographic studies (Table IV).[32,33] The EXAFS analyses of **1a,b** and **2b** in methanol indicated that there is no dramatic change around the metal center on dissolution in methanol. As to complex **2a** in the solid state, the abstracted EXAFS oscillation was fitted by the four-term equation of $k^3\chi_{calcd}(k) = k^3[\chi_{N/O}(k) + \chi_{Cl_{eq}}(k) + \chi_{Cl_{ax}}(k) + \chi_C(k)]$, in accordance with the crystal structure. Although the backscattering contribution of the chlorine atom in the equatorial plane (Cl$_{eq}$) was weak and was concealed in the intense first shell peak, the contribution can be confirmed by the difference Fourier transformation of $k^3\chi_{obsd}(k) - k^3[\chi_{N/O}(k) + \chi_{Cl_{ax}}(k) + \chi_C(k)]$ (dotted line) (Figure 4d). In the Fourier transform of **2a** in methanol, the contribution of the chlorine atom in the axial position was not observed in spite of some attempts of curve-fitting analyses (Figure 4c), suggesting that the axial chloride ion is likely to dissociate in solution to generate essentially square planar species. The Fourier transform and curve-fitting analysis of [Cu$_2$(*N,N,N',N'*-Me$_4$en)$_2$(OH)$_2$]Br$_2$ (**6**) demonstrated that Cu···Cu interactions with μ-hydroxo bridgings around 3 Å are clearly observable in EXAFS spectroscopy.

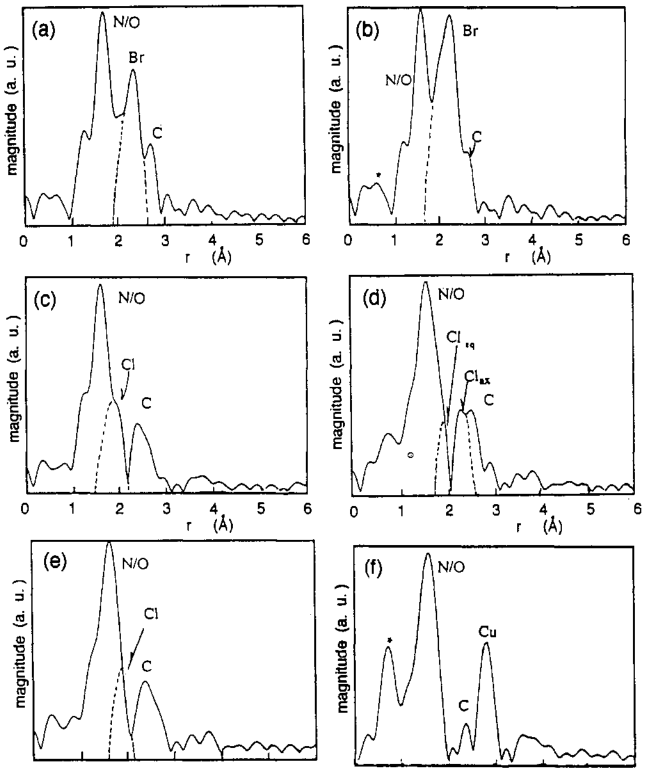

Figure 4. Fourier transforms for (a) Cu(hen(OH))Br$_2$ (**1b**, powder), (b) Cu(hen(OH)$_2$)Br$_2$ (**2b**, powder), (c) Cu(hen(OH))Cl$_2$ (**1a**, powder), (d) Cu(hen(OH)$_2$)Cl$_2$ (**2a**, powder), (e) **2a** in methanol, and (f) [Cu$_2$(OH)$_2$(*N,N,N',N'*-Me$_4$en)$_2$]Br$_2$ (**6**, powder).

X-ray Absorption Analyses and the Proposed Structure of Copper(II) Complexes Containing *N*-Glycosides. Figure 6 shows XANES spectra of the complex **3a** in the solid (a) and solution (b) states together with those of **1a** (powder) (c) and **2a** (solution) (d). On the basis of the recent understanding of XANES spectra of copper(II) complexes,[34] the feature labeled A could be assigned

---

(33) It should be noted that the semicoordination structure of the halogen atoms cannot be characterized at all in the present EXAFS analyses.

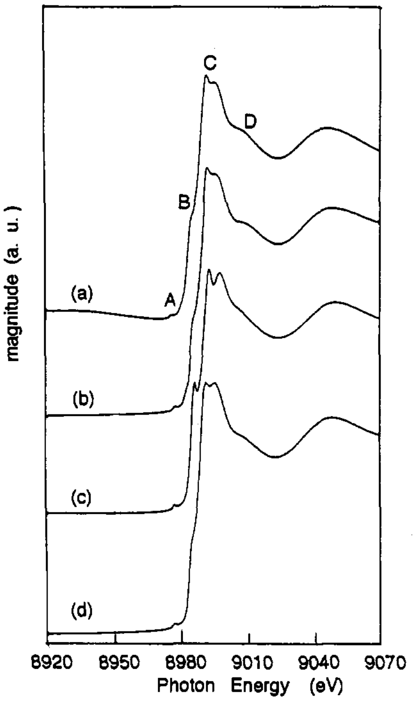

Figure 6. Normalized X-ray absorption spectra around Cu K edge for (a) Cu(*N*,*N*′-(D-Glc)$_2$-en)Cl$_2$ (**3a**, powder), (b) **3a** in methanol, (c) Cu(hen(OH))Cl$_2$ (**1a**, powder), and (d) Cu(hen(OH)$_2$)Cl$_2$ (**2a**, in methanol).

to a 1s → 3d quadrupolar allowed transition (8979 eV),[35] B to a vibronically allowed 1s → 4s transition[36] or a 1s → 4p transition simultaneous with ligand to metal shakedown (8986 eV),[37–39] and C to a 1s → 4p transition[38,39] or a 1s → continuum resonance (8990–9000 eV),[40] respectively. The feature D has generally been understood as arising from continuum resonances involving multiple-scattering effects. These features of **3a** found in both solid and solution states are closely similar to those of Cu(hen(OH)Cl$_2$ (**1a**, powder) and Cu(hen(OH)$_2$)Cl$_2$ (**2a** in methanol), showing the similarity of the structure around the metal between these complexes. The XANES spectra of other sugar complexes (**3–5**) and reference compounds (**1b** and **2b**) showed almost identical patterns except for some broadenings of peaks.

The Fourier transforms of $k^3\chi(k)$ of the copper(II) *N*-glycosides complexes are given in Figure 7. The Fourier-filtered $k^3\chi(k)$ oscillations, produced by back-Fourier transformation of *r* peaks in the range 1–3 Å, were successfully analyzed by curve-fitting techniques using the three-term equation of $k^3\chi_{\text{calcd}}(k) = k^3[\eta_{\text{N/O}}(k) + \chi_{\text{Cl,Br}}(k) + \chi_{\text{C}}(k)]$. Representative curve-fitting results for **3a** and **4c** are shown in Figure 8.[32] The back-scattering contributions of the chlorine atoms directly coordinating to the Cu atom were apt to be concealed in the intense peak of the first shell atoms, so we confirmed their contributions by the difference Fourier transformation of $k^3\chi_{\text{obsd}}(k) - k^3[\chi_{\text{N/O}}(k) + \chi_{\text{C}}(k)]$ (dotted lines). The structural parameters derived from the EXAFS analyses are summarized in Table V.[32] These results exhibited that the central copper atoms is surrounded by three nitrogen and/or oxygen atoms (r = 1.95–2.02 Å, N = 2.0–3.8) and one halogen atom (Cl, r = 2.22–2.30 Å, N = 0.7–1.3; Br, r = 2.33–2.45 Å, N = 0.8–1.2), similar to the reference complexes (except for **2a** in crystalline form).[33] The EXAFS analyses of the solution samples (**3a,e**, **4a,c**) also did not show significant structural change around the metal center.

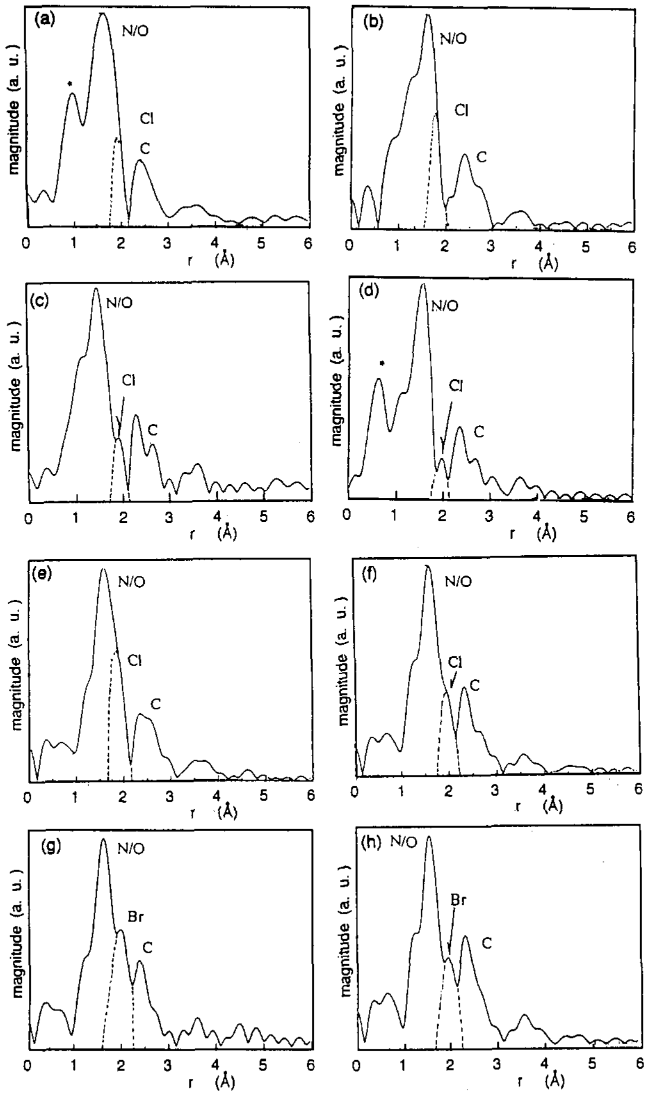

Figure 7. Fourier transforms for (a) Cu(*N*,*N*′-(D-Glc)$_2$-en)Cl$_2$ (**3a**, powder), (b) Cu(*N*,*N*′-(D-Man)$_2$-en)Cl$_2$·Solv (**3b**, powder), (c) Cu(*N*-(D-Glc)-*N*,*N*′-Me$_2$en)Cl$_2$·Solv (**4a**, powder), (d) Cu(*N*-(D-Man)-*N*,*N*′-Me$_2$en)Cl$_2$·Solv (**4b**, powder), (e) Cu(*N*′-(D-Glc)-*N*,*N*-Me$_2$en)Cl$_2$·Solv (**5a**, powder), (f) Cu(*N*,*N*′-(D-Glc)$_2$-en)Br$_2$·Solv (**3e**, powder), and (h) Cu(*N*-(D-Glc)-*N*,*N*′-Me$_2$en)Br$_2$·Solv (**4c**, powder).

On the basis of analytical and AB and CD spectral data as well as the results of X-ray absorption analyses, the copper(II) *N*-glycosides complexes were assumed to have the mononuclear structure as depicted in Figure 9. Complex **3** is square planar, and the central copper atom is coordinated by a halide ion (Cl$^-$ or Br$^-$) and a tridentate *N*-glycoside ligand, *N*,*N*′-(β-D-aldose)$_2$-en, through the two nitrogen atoms of the diamine moiety and the oxygen atom of hydroxy group on the C-2 position of a sugar unit. The other sugar moiety does not form a distinct bond with the central copper(II) ion (Figure 9a,b). The D-glucopyranoside unit having an *R* configuration around the C-2 carbon tentatively forms a λ-*gauche* five-membered chelate ring, and the pyraonoid ring is included in the equatorial plane (Figure 9a); in contrast, the D-mannopyranoside unit having an *S* configuration around the C-2 carbon forms a δ-*gauche* chelate ring. The pyranoid ring is significantly raised out of the equatorial plane (Figure 9b). Complexes **4** and **5** were also presumed to have similar structures around the metal center; a tridentate *N*-glycoside ligand, *N*-(β-D-aldose)-*N*,*N*′-Me$_2$en or *N*′-(β-D-aldose)-*N*,*N*-Me$_2$en, coordinates to the copper via the two nitrogen atoms of the diamine and

---

(34) Strange, R. W.; Alagna, L.; Durham, P.; Hasnain, S. S. *J. Am. Chem. Soc.* **1990**, *112*, 4265.

(35) Schlman, R. G.; Yafet, T.; Eisenberger, P.; Blumberg, W. E. *Proc. Natl. Acad. Sci. U.S.A.* **1976**, *73*, 1384.

(36) Chan, S. I.; Hu, V. W.; Gamble, R. C. *J. Mol. Struct.* **1978**, *45*, 239.

(37) Blair, R. A.; Goddard, W. A. *Phys. Rev.* **1980**, *b22*, 2767.

(38) Kosugi, N.; Yokoyama, T.; Asakura, K.; Kuroda, H. *Chem. Phys.* **1984**, *91*, 249.

(39) Yokoyama, T.; Kosugi, N.; Kuroda, H. *Chem. Phys.* **1986**, *103*, 101.

(40) Smith, T. A.; Berding, M.; Penner-Hahn, J. E.; Doniach, S.; Hodgson, K. O. *J. Am. Chem. Soc.* **1985**, *107*, 5945.

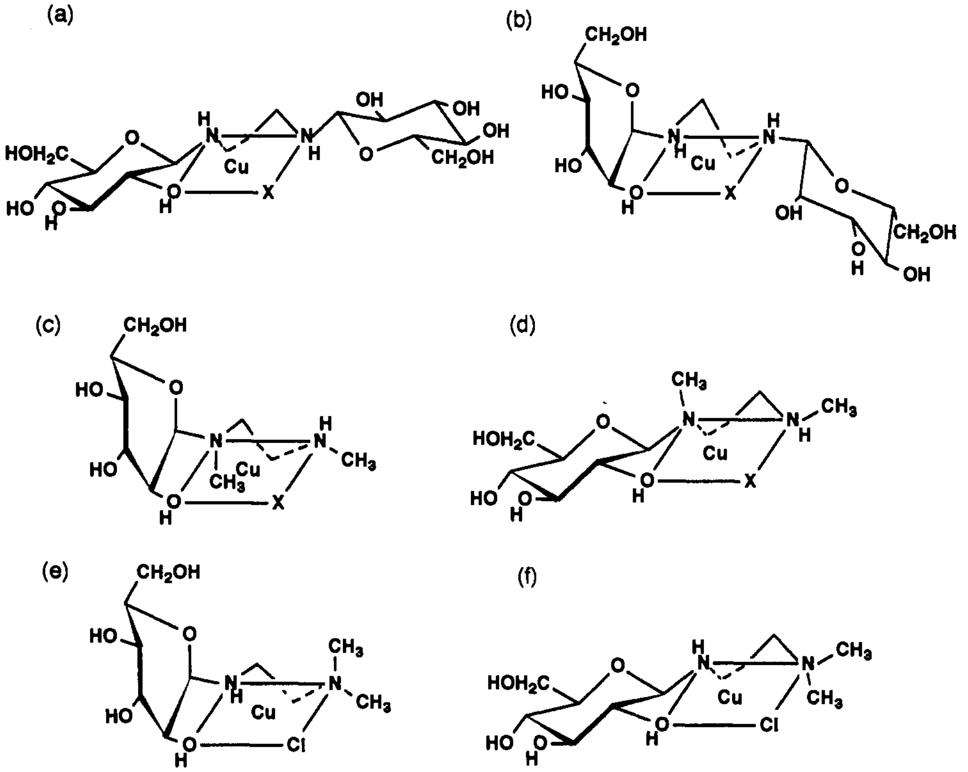

Figure 9. Proposed structures of the complex cations for (a) $[Cu(N,N'\text{-}(\text{D-Glc})_2\text{-en})X]^+$ (**3a,e**), (b) $[Cu(N,N'\text{-}(\text{D-Man})_2\text{-en})X]^+$ (**3b,f**), (c) $[Cu(N\text{-}(\text{D-Man})\text{-}N,N'\text{-Me}_2\text{en})X]^+$ (**4b,d**), (d) $[Cu(N\text{-}(\text{D-Glc})\text{-}N,N'\text{-Me}_2\text{en})X]^+$ (**4a,c**), (e) $[Cu(N'\text{-}(\text{D-Man})\text{-}N,N\text{-Me}_2\text{en})Cl]^+$ (**5b**), and (f) $[Cu(N'\text{-}(\text{D-Glc})\text{-}N,N\text{-Me}_2\text{en})Cl]^+$ (**5a**). X = Cl^- or Br^-.

the oxygen atom of the C-2 hydroxy group of the carbohydrate unit (Figure 9c–f).

Catalytic Epoxidation of Olefins by the Copper(II) Complexes Containing *N*-Glycoside Ligands. Epoxidation of olefins is an important reaction in organic synthesis because epoxides are intermediates that can be converted to a variety of organic compounds.[41] In particular, chiral epoxides play an attractive role as building blocks in the synthesis of natural products. Groves et al. have studied asymmetric epoxidations of olefins catalyzed by iron complexes of porphyrins containing axially asymmetric binaphthyl moieties,[24,42] and recently, Jacobsen et al. reported an enantioselective epoxidation of unfunctionalized olefins by manganese complexes of chiral Shiff bases.[43]

Naturally abundant carbohydrates are easily available chiral source and are potential ligands in asymmetric catalytic reactions. However, no attempt of their use in epoxidation of olefins has been made thus far. In this respect, we investigated an epoxidation of olefins by the copper(II) complexes of *N*-glycosides.[44]

The reaction was carried out by addition of oxidant (*tert*-butyl hydroperoxide (TBHP) or iodosylbenzene (PhIO)) to a solution of the copper(II) *N*-glycoside complex and olefin in acetonitrile under a nitrogen atmosphere. The reaction mixture was stirred continuously at room temperature, and the products were monitored by GC or HPLC. The results are summarized in Table VI. The sugar complex (**3a**,**b**, **4a**,**b**, **5a**,**b**)–TBHP system catalyzed the epoxidation of unfunctionalized olefin, (*E*)-β-methylstyrene, to give corresponding oxide (18–47% yield), but the system of the sugar complex–PhIO did not promote the epoxidation; the starting olefin was recovered quantitatively. The time course of the reaction of (*E*)-β-methylstyrene mediated by **3a** is given in Figure 10. The yield of oxide was saturated at 47%, while the conversion of (*E*)-β-methylstyrene reached 95%. This indicated that some side reactions occurred during the epoxidation, but their products were not determined in the present study. Dichloromethane was useful as a solvent, but the reaction was substantially interrupted in DMF and MeOH. (*Z*)- and (*E*)-Stilbene were found to be more reactive than (*E*)-β-methylstyrene, and the product in both cases was (*E*)-stilbene oxide. In all cases, the enantioslectivities for epoxides of unfunctionalized olefins were extremely low (ee 0–7%), probably due to poor interaction between hydroxy groups of the sugar unit and nonpolar substrate.

Table VI. Epoxidation of Olefins Promoted by Copper(II) N-Glycoside Complexes

catal.	substrate[a]	solvent	oxidant	yield of epoxide, %[b]
3a	(*E*)-β-methylstyrene	CH_3CN	TBHP	47
3a	(*E*)-β-methylstyrene	CH_3CN	PhIO	0
3a	(*E*)-β-methylstyrene	CH_2Cl_2	TBHP	45
3a	(*E*)-β-methylstyrene	DMF	TBHP	7
3a	(*E*)-β-methylstyrene	CH_3OH	TBHP	4
3b	(*E*)-β-methylstyrene	CH_3CN	TBHP	43
4a	(*E*)-β-methylstyrene	CH_3CN	TBHP	38
4b	(*E*)-β-methylstyrene	CH_3CN	TBHP	18
5a	(*E*)-β-methylstyrene	CH_3CN	TBHP	38
5b	(*E*)-β-methylstyrene	CH_3CN	TBHP	23
3a[c,d]	(*E*)-stilbene	CH_3CN	TBHP	52[e]
3a[d]	(*Z*)-stilbene	CH_3CN	TBHP	78[e,f]
3a	(*E*)-cinnamyl acetate	CH_3CN	TBHP	24
3b	(*E*)-cinnamyl acetate	CH_3CN	TBHP	22

[a] Substrate was treated with oxidant and a catalytic amount of copper(II) complex (2 mol %) in acetonitrile at room temperature for 80 h. [b] Based on substrate determined by GC. [c] 10 mol % vs substrate. [d] Reaction time is 100 h. [e] Determined by HPLC. [f] (*E*) isomer.

Some olefins involving functional groups were examined. Whereas allyl alcohol, (*E*)-cinnamyl alcohol, and (*E*)-benzal acetone were not converted to the corresponding epoxides, (*E*)-cinnamyl acetate was transformed to the oxide in low yields (by **3a** or **3b**). Interestingly, using **3b**, which contains D-mannose

---

(41) Jorgensen, K. A. *Chem. Rev.* **1989**, *89*, 431.

(42) Groves, J. T.; Viski, P. *J. Org. Chem.* **1990**, *55*, 3628.

(43) Zhang, W.; Loebach, J. L.; Wilson, S. R.; Jacobsen, E. N. *J. Am. Chem. Soc.* **1990**, *112*, 2801.

(44) The epoxidation of olefins by copper(II) salts or copper(II) complex–PhIO systems has been already reported: (a) Franklin, C. C.; VanAtta, R. B.; Tai, A. F.; Valentine, J. S. *J. Am. Chem. Soc.* **1984**, *106*, 814. (b) VanAtta, R. B.; Flanklin, C. C.; Valentine, J. S. *Inorg. Chem.* **1984**, *23*, 4121. (c) Tai, A. F.; Margerum, L. D.; Valentine, J. S. *J. Am. Chem. Soc.* **1986**, *108*, 5006.

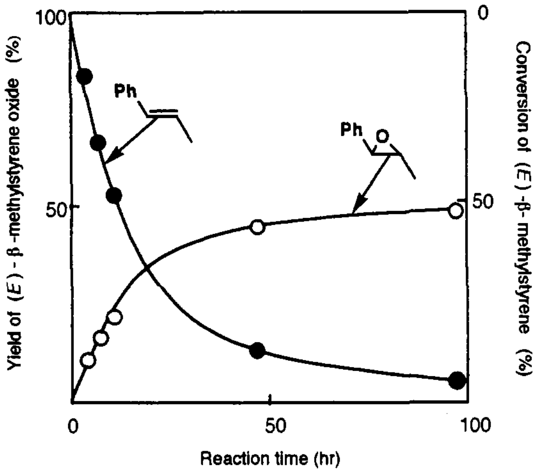

Figure 10. Reaction profile for the epoxidation of (*E*)-β-methylstyrene with TBHP catalyzed by Cu(N,N'-(D-Glc)$_2$-en)Cl$_2$ (**3a**): (○) (*E*)-β-methylstyrene oxide; (●) (*E*)-β-methylstyrene.

unit, the enantioselectivity increased to ee 16% ((+)-enantiomer rich), in contrast with an extremely low ee (~0%) for **3a** containing the D-glucose unit. This might indicate the importance of some interactions between the sugar unit and substrate around the metal center. On the basis of the structure of **3**, D-mannose-containing complex **3b** seems to be preferable for such an interaction. Anyhow, this is the first example of catalytic reactions mediated by transition metal complexes containing free sugar moieties, though the detailed mechanistic aspects for the asymmetric induction were not elucidated at present. Studies along this line are now in progress.

Acknowledgment. This work was partially supported by a Grant-in-Aid for Scientific Research from the Ministry of Education, Science, and Culture of Japan (No. 02740306).

Supplementary Material Available: Listings of crystallographic parameters, atomic coordinates, anisotropic thermal parameters, and bond distances and angles for **1a,b** and **2a,b**, listings of EXAFS and X-ray atomic parameters (Tables IV and V), figures showing the results of curve-fitting (observed and calculated EXAFS oscillations), and figures showing the structures of **1a,b** and **2a,b** and additional curve fittings (Figures 3, 5, and 8) (32 pages). Ordering information is given on any current masthead page.